UPLC-QTOFMS^{E}-Guided Dereplication of the Endangered Chinese Species *Garcinia paucinervis* to Identify Additional Benzophenone Derivatives

By: Ping Li, Harini Anandhi Senthilkumar, Mario Figueroa, Shi-Biao Wu, Jimmie E. Fata, Edward J. Kennelly, Chunlin Long

Li, P., Anandhi Senthilkumar, H., Figueroa, M., Wu, S.-B., Fata, J.E., Kennelly, E.J., Long, C. (2016). UPLC-QTOFMS^{E}-Guided Dereplication of the Endangered Chinese Species *Garcinia paucinervis* to Identify Additional Benzophenone Derivatives, *Journal of Natural Products, 79* (6), pp. 1619-1627. DOI: 10.1021/acs.jnatprod.6b00186

Abstract:

A number of *Garcinia* species accumulate benzophenone derivatives that may be useful for the treatment of breast cancer. The dereplication of new benzophenone derivatives from *Garcinia* species is challenging due to the occurrence of multiple isomers and the known compounds found in their extracts. In the current study, a strategy is described using the UPLC-QTOFMS^{E} technique to identify tentatively the known and uncharacterized benzophenones of interest based upon the characteristic fragmentation ions. Several UPLC-QTOFMS peaks (*a*–*ee*) appeared to contain benzophenone derivatives, and 12 of these peaks contained compounds with MS ionization profiles not consistent with previously identified compounds from the seeds of *Garcinia paucinervis*, an endangered Chinese species. The targeted isolation of unidentified compounds of interest afforded five new benzophenones, paucinones E–I (**1**–**5**), which were determined by MS and NMR analysis and ECD spectroscopy. These compounds were evaluated for cytotoxicity against three breast cancer cell lines inclusive of MDA-MB-231, SKBR3, and MCF-7. These results indicate that the UPLC-QTOFMS^{E}-guided isolation procedure is an efficient strategy for isolating new benzophenones from *Garcinia* species.

Keywords: benzophones | breast cancer treatment | *Garcinia paucinervis*

Article:

Most benzophenones characterized from *Garcinia* species are representative of two main classes of compounds, the polyisoprenylated benzophenones (PIBs) and polycyclic polyprenylated acylphloroglucinols (PPAPs), and their structures usually contain a number of prenyl or geranyl groups, hydroxy groups, and complex ring systems. The PIBs and PPAPs have exhibited biological activities inclusive of cytotoxic effects on human cancer cell lines and antibacterial, anti-HIV, anti-inflammatory, and antioxidant effects.(1-7) Benzophenone derivatives from *Garcinia* species are recognized for their structural diversity and significant biological activity, leading to the discovery of many new compounds.(8, 9)

Conventional activity-guided isolation from medicinal plants often requires kilogram amounts of plant material and is both laborious and costly. Due to the structural similarity among the *Garcinia* benzophenone derivatives, it can be challenging to separate and identify those analogues.(10) LC-MS/MS-guided isolation affords fragment ions that can be used in the structural elucidation of plant metabolites and has been demonstrated to increase the efficiency for natural products discovery.(11-14) This technique has also been used successfully to profile the diagnostic daughter ions of PPAPs and PIBs.(10, 15, 16) However, MS/MS experimental analysis needs specific precursor ion selection and repeated injections of samples, thus being cumbersome when thousands of metabolic constituents are included in an analysis. In recent years, the UPLC-QTOFMS^E technique was highlighted to assess the highly sensitive and rapid analysis of complex multicomponent mixtures.(17) In particular, MS^E spectrometric data with parallel alternating scans are acquired at either low collision energy to obtain precursor ion information or high collision energy to generate the precursor ion and fragment ions, providing similar information to conventional MS/MS from a single analytical run.(18, 19) This powerful tool can be useful for the characterization and identification of different classes or types of natural products, including PPAPs and PIBs.

Garcinia paucinervis Chun & F. C. How (Clusiaceae) is an endemic species to mainland China, distributed mainly in southwest provinces such as Guangxi and Yunnan. It provides valued hardwood, resulting in its being overharvested, and is now considered a Class II endangered species in mainland China. In addition to its useful wood, the roots, leaves, and bark can also be used as folk medicine for the treatment of bacterial skin infections, bruises, and burns.(20)*G. paucinervis* is known to produce many benzophenones that have biological activity. For example, the benzophenone derivatives paucinones A–D, isolated from the leaves of this species, showed cytotoxicity against HeLa cells.(21) Currently, there have been over 50 compounds including 20 benzophenone derivatives reported from this species.(20-23)

In the past decade, our laboratory has isolated and identified a number of *Garcinia* prenylated benzophenones with cytotoxic activity.(24-28) An interest is retained in cytotoxic benzophenones from additional *Garcinia* species, to better understand their structure–activity relationships. This report is focused on *G. paucinervis*, to better understand the considerable chemical diversity from this endangered species. A UPLC-QTOFMS^E strategy was used to identify benzophenone derivatives from the fractions of *G. paucinervis* seeds. Five new benzophenones (**1**–**5**) were isolated, and their structures were elucidated with NMR, IR, and electronic circular dichroism (ECD) spectra. In addition, their cytotoxic effects on three clinically relevant breast cancer cell lines, MDA-MB-231, SKBR3, and MCF-7, were evaluated.

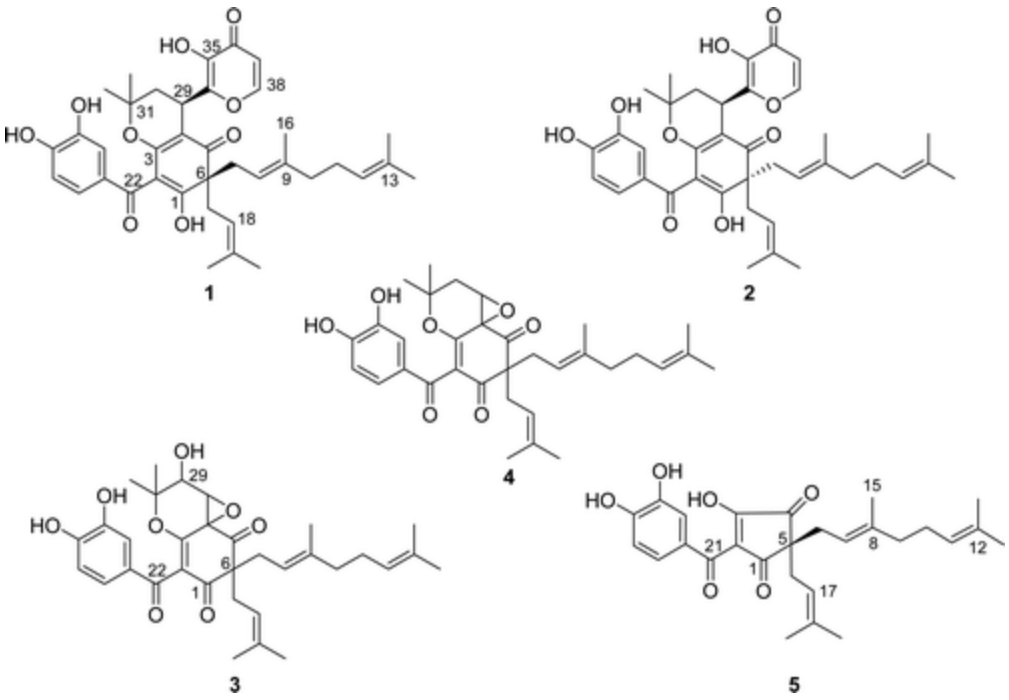

Chart 1

Results and Discussion

An ethanol extract of *G. paucinervis* seeds was defatted with petroleum ether, and the defatted residue was then chromatographed over a column containing silica gel to yield nine fractions. All fractions were analyzed by UPLC-QTOFMS, using two modes: (1) an MS full scan, to obtain the accurate molecular formulas of detected peaks; and (2) an MS^E experiment, to produce fragment ions to deduce the potential benzophenone derivates. The benzophenone derivatives were detected in nine fractions, and 31 peaks (*a–ee*) from these fractions were identified as containing potential benzophenone derivatives, as supported by the molecular formula, by the diagnostic fragment ion (*m*/*z* 177.02),(10) and compared to the *Garcinia* compounds previously indexed in the SciFinder database (Chemical Abstracts Service, Columbus, OH, USA). Among them, 19 peaks were judged to contain known benzophenones, including a number of isomers often with similar fragment ions. For instance, peaks *o–s* ($C_{38}H_{50}O_7$), peaks *u–w*, *z–bb* ($C_{38}H_{48}O_6$), and peaks *x*, *cc–ee* ($C_{38}H_{50}O_6$) were previously reported in *Garcinia* species (Table S1, Supporting Information). The other 12 peaks contained compounds that were classified tentatively as benzophenones, due to the loss of prenylated groups, benzene rings, and the diagnostic ion at *m*/*z* 177.0188 ($C_9H_5O_4$) observed in the MS^E spectrum. On the basis of the comprehensive analysis of these 12 peaks, the basic structural units of six compounds were proposed, and these were considered to be “unknowns of interest”, warranting further isolation and identification work.

Peak *g* (t_R = 3.60 min) eluted closely with peak *h* (t_R = 3.73 min), only observed in fraction E, which could be identified as isomeric compounds ($C_{38}H_{44}O_9$), due to both displaying the same molecular ions at *m*/*z* 645.3070 $[M + H]^+$ and 643.2901 $[M – H]^–$. For peak *g*, the MS^E spectra are shown in Figure 1, with the molecular ions and the main fragment ions obtained under the low-energy mode. The fragment ion at *m*/*z* 509.1809 corresponded to the loss of two prenyl

groups ($2C_5H_8$) from the molecular ions, and it lost a further C_5H_8 unit to produce an ion at *m*/*z* 453.1179. While additional ion fragments could be observed in the high-energy mode, a continuous loss of $C_5H_4O_3$, C_5H_8, C_4H_8, and $C_6H_6O_2$ suggested another ion pathway in peak *g*. Such a molecular formula and the basic structure units have not been found previously in *Garcinia* metabolites. Thus, both peaks *g* and *h* were targeted as potentially containing unknown benzophenone-type structures. Peaks *e* and *f* ($C_{33}H_{40}O_8$) and peak *b* ($C_{27}H_{32}O_6$) were also further investigated, using similar reasoning (Figures S1 and S2, Supporting Information).

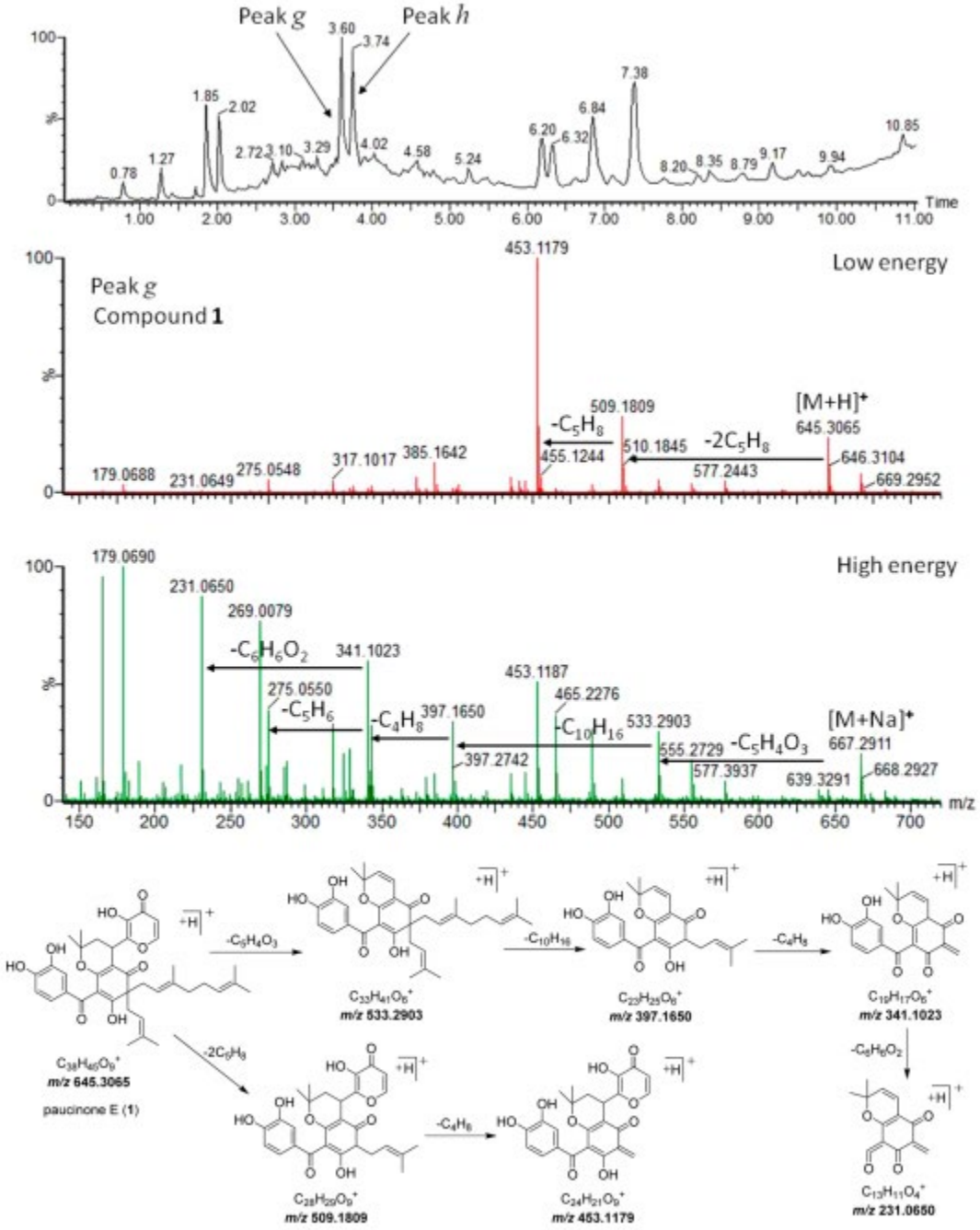

Figure 1. HRMS^E spectra and proposed fragmentation pathway of paucinone E (**1**).

Based on UPLC-QTOFMS^E fragment ion analysis on the peaks of the nine *G. paucinervis* fractions, six target peaks (*b*, *e*, *f*, *l*, *g*, and *h*) were considered unknowns of interest. They were separated by Sephadex LH-20 chromatography and semipreparative HPLC to obtain compounds **1**–**5**. The details of isolation are described in the Experimental Section. Their structures are assigned by the means of NMR, MS, IR, and ECD spectroscopy.

Paucinones E (**1**) and F (**2**) were obtained as yellow, amorphous powders from peaks *g* and *h*, respectively, and had the same molecular formula $C_{38}H_{44}O_9$ by HRQTOFMS (*m/z* 645.3070 [M + H]$^+$ and *m/z* 645.3063 [M + H]$^+$, calcd 645.3064), representing a hydrogen index deficiency of 17, and their ^{1}H, ^{13}C, and 2D NMR spectroscopic data were almost identical. The ^{1}H NMR spectrum for **1** exhibited seven methyl groups signals [δ_H 1.01, 1.19, 1.51, 1.55, 1.56, 1.62, and 1.64], two olefinic proton signals [δ_H 7.8 (1H, d, *J* = 5.5 Hz) and 6.4 (1H, d, *J* = 5.5 Hz)], and signals for a trisubstituted aromatic ring [δ_H 7.10 (1H, d, *J* = 2.1 Hz), 7.04 (1H, dd, *J* = 8.2, 2.1 Hz), and 6.78 (1H, d, *J* = 8.2 Hz)] (Table 1). The ^{13}C NMR and DEPT spectra of **1** revealed the presence of 38 carbon atoms, including three carbonyl carbons, five methylenes, nine methines (eight olefinic), seven methyl groups, and 14 quaternary carbons (two sp^3 quaternary carbons). The HSQC and HMBC spectra demonstrated that **1** contains a trisubstituted aromatic ring, three carbonyls, and three prenyl groups. All these moieties indicated that **1** is a prenylated benzophenone derivative.(1) The diagnostic chemical shift (δ_C 41.1) for C-10 in the ^{13}C NMR spectrum indicated the 10*E* geometry in compound **1** as supported by a previous report.(29) In addition, H-7 exhibited correlations with the C-6, C-5, and C-9 carbons in the HMBC spectrum and allowed the assignment of the geranyl group at the C-6 position. Another prenylated unit was attached to the C-6 carbon as well, as supported by the HMBC correlations between protons H-17 and C-6, C-1, C-7, and C-19. The core structure of **1** (C-1 to C-18) agreed closely with previously reported kolanone analogues,(30, 31) isolated from *G. kola* Heckel seeds. However, compound **1** had an additional cyclohexane oxide ring attached at C-3 and C-4, shown by the HMBC correlations between H-29/C-3 (δ_C 169.3), H-30/C-4 (δ_C 105.3), and Me-32 and Me-33/C-30 (δ_C 37.4) and C-31 (δ_C 79.7), respectively. The remaining five carbons (δ_C 156.7, 144.0, 175.5, 114.6, and 155.6) and ^{1}H–^{1}H COSY correlation of H-37/H-38 were in agreement with the pyromeconic acid group,(32) which is attached at C-29, as supported by the key HMBC correlations of H-29/C-34 and H-30/C-34 (Figure 2), thereby defining the planar structure of compound **1** as defined.

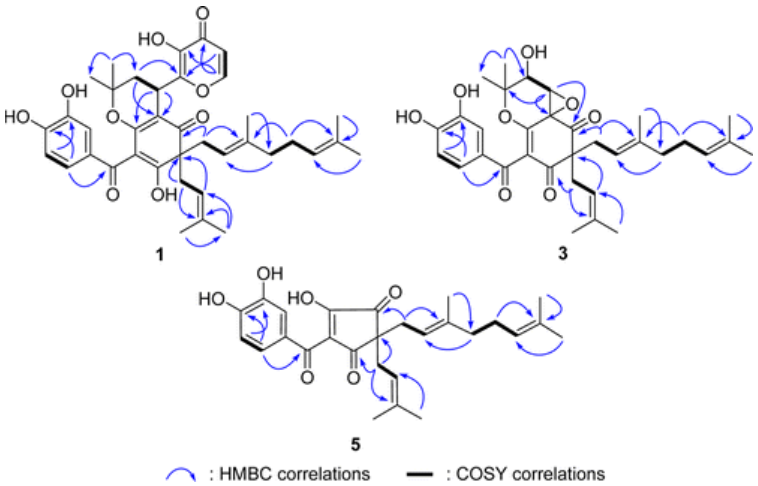

Figure 2. Key COSY and HMBC of paucinone E (**1**), paucinone G (**3**), and paucinone I (**5**).

Table 1. NMR Spectroscopic Data (300 MHz, CD_3OD) for Compounds 1–3

	1		2		3a		3b	
position	δ_C	δ_H (*J* in Hz)	δ_C	δ_H (*J* in Hz)	δ_C	δ_H (*J* in Hz)	δ_C	δ_H (*J* in Hz)
1	189.5		189.2		197.5		197.5	
2	109.4		109.4		128.4		128.3	
3	169.3		169.8		164.3		164.1	
4	105.3		105.6		55.8		55.7	
5	197.6		197.6		204.6		204.6	
6	60.2		60.1		66.5		66.5	
7	39.0	2.74, 2.51, m	39.6	2.70, 2.48, m	37.6	2.64, 2.56, m	37.3	2.63, 2.55, m
8	119.6	4.95, m	119.9	4.96, m	119.4	4.98, m	119.3	4.99, m
9	139.5		139.9		141.5		141.0	
10	41.2	1.96, m	41.1	1.94, 1.96, m	41.2	2.02, 1.96, m	41.2	2.00, 1.95, m
11	27.9	2.01, 1.93, m	27.9	2.01, 1.93, m	28.1	2.09, 1.99, m	27.8	2.07, 1.97, m
12	125.3	5.08, m	125.2	5.03, m	125.1	5.11, m	125.0	5.08, m
13	132.5		132.5		132.7		132.7	
14	26.1	1.62, s	26.1	1.64, s	26.1	1.66, s	26.1	1.66, s
15	18.0	1.55, s	18.0	1.56, s	18.0	1.59, s	18.0	1.59, s
16	16.7	1.54, s	16.7	1.58, s	16.8	1.57, s	16.6	1.57, s
17	40.1	2.64, 2.57, m	39.7	2.68, 2.54, m	39.3	2.67, 2.50, m	39.2	2.65, 2.49, m
18	119.4	4.94, m	119.4	4.92, m	118.9	5.03, m	118.5	5.02, m
19	136.5		135.6		137.9		137.3	
20	26.4	1.64, s	26.5	1.67, s	18.2	1.55, s	18.2	1.55, s
21	18.2	1.56, s	18.2	1.51, s	26.4	1.70, s	26.4	1.70, s
22	193.0		193.6		193.3		193.3	
23	131.9		132.3		130.5		130.5	
24	117.0	7.10, d (2.1)	117.0	7.14, d (2.1)	116.3	7.36, d (2.1)	116.2	7.36, d, (2.1)
25	146.0		146.0		147.0		147.0	
26	151.3		151.3		153.2		153.2	
27	115.2	6.78, d (8.2)	115.3	6.77, d (8.2)	115.7	6.78, d (8.3)	115.7	6.77, d (8.3)
28	123.7	7.04, dd (8.2, 2.1)	123.9	7.07, dd (8.2, 2.1)	125.3	7.17, dd (8.3, 2.1)	125.2	7.17, dd (8.3, 2.1)
29	30.5	4.16, dd (11.2, 6.7)	30.6	4.15, dd (10.9, 6.9)	63.7	4.27, d (1.2)	63.7	4.28, d (1.3)
30	37.4	2.02, 1.89, m	37.2	2.02, 1.89, m	70.9	4.00, d (1.2)	70.9	3.96, d (1.2)
31	79.7		79.5		87.0		86.8	
32	28.4	1.01, s	28.4	1.01, s	29.2	1.20, s	29.2	1.20, s
33	23.9	1.19, s	24.2	1.19, s	23.7	1.38, s	23.6	1.38, s
34	156.7		156.9					
35	144.0		144.0					
36	175.5		175.6					
37	114.6	6.40, d (5.5)	114.6	6.41, d (5.5)				
38	155.6	7.80, d (5.5)	155.8	7.88, d (5.5)				

The ^{1}H NMR spectrum for **2** also exhibited signals for seven methyl groups, one olefinic proton, and one trisubstituted aromatic ring (Table 1). The differences between compounds **1** and **2** involve the chiral carbons at C-6 and C-29. Compounds **1** and **2** exhibited opposite signs for optical rotation values [**1**, +66, and **2**, −74] and almost mirror-image ECD spectra (Figure 3). On the basis of the fact that these compounds were separated by a nonenantioselective method, compounds **1** and **2** were not considered as being enantiomers but rather diasteroisomers. Since NOESY data were not useful in establishing the relative configurations of **1** and **2** at these chiral atoms, their absolute configurations were established by comparison of their experimental and calculated ECD spectra, as predicted by the time-dependent density functional theory (TDDFT) approach.(27, 33-36) Molecular modeling

calculations, such as ECD and optical rotation, have been used to determine the absolute configuration of prenylated benzophenones.(27) Thus, a Monte Carlo conformational search using the MMFF94 molecular mechanics force field was perform for diasteroisomers 6*S*, 29*R* and 6*R*, 29*R* (Figure S3, Supporting Information). For this, and to minimize computational time, the aliphatic chains at C-6 were reduced to a methyl group and hydrogen due to the numerous conformations generated in the conformational analysis with little or no effect on the ECD calculations.(37) The enantiomers 6*R*, 29*S* and 6*S*, 29*S* were not computed since the ECD-calculated spectra are antipodal. Then, each conformer was geometrically optimized at the B3LYP/DGDZVP level of theory (Figure S3, Supporting Information) with the polarizable continuum model (PCM) for methanol, as implemented in the Gaussian 09 software. The Boltzmann-averaged ECD spectra of diasteroisomers 6*S*, 29*R* and 6*R*, 29*R* (Figure 3) based on TDDFT showed an excellent fit with the experimentally measured data: (a) diasteroisomer 6*S*, 29*R* showed negative Cotton effects at 260 and 350 nm and a positive Cotton effect at 300 nm, which was in good agreement with the experimental data for compound **1**; (b) diasteroisomer 6*R*, 29*R* showed a positive Cotton effect at 250 nm and a negative Cotton effect at 330 nm, which was in good agreement with the experimental data for compound **2**. Thus, the absolute configurations of compounds **1** and **2** were determined as 6*S*, 29*R* and 6*R*, 29*R*, respectively.

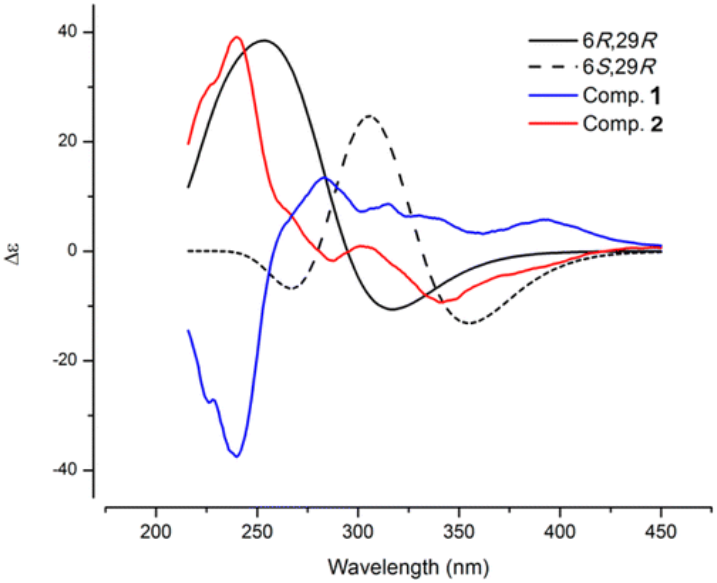

Figure 3. Experimentally measured ECD spectra of compounds (A) and calculated ECD spectra (B) of paucinones E (**1**, 0.78 mM, MeOH, cell length 2 cm) and F (**2**, 0.78 mM, MeOH, cell length 2 cm).

Paucinone G (**3**) was obtained from peaks *e* and *f*, as a yellow, amorphous powder. Its molecular formula was assigned as $C_{33}H_{40}O_8$, based on the ^{13}C NMR data and the molecular ion peaks in the HRQTOFMS (*m*/*z* 565.2803 $[H + M]^+$, calcd for 565.2801, $C_{33}H_{41}O_8$), and represented 14 degrees of unsaturation. From the ^1H NMR spectrum of **3**, seven methyl groups and one trisubstituted aromatic ring were observed (Table 1). The ^{13}C NMR and DEPT spectra of **3** accounted for 33 carbons, classified as three carbonyls, four methylenes, eight methines, seven methyl groups, and 11 quaternary carbons, showing close similarities to those of **1**, thus suggesting that compound **3** is also a prenylated benzophenone. On comparison of the 1D and 2D NMR spectra of **3** and **1**, the obvious differences were that (1) the signals of a pyromeconic

acid group were not observed in **3** and (2) there was a carbonyl (δ_C 197.5) at C-1 of **3**, as supported by the HMBC correlations of H-7 and H-17/C-1, C-5, and C-6. Furthermore, a 2,2-dimethyl-3-hydroxypyran moiety was assigned at C-3 and C-4, as confirmed by the HMBC correlations between H-29/C-4, C-5 and C-31, H-30/C-4 and C-29, Me-32/C-31 and C-33, and Me-33/C-30 and C-31. Other key HMBC and ^{1}H–^{1}H COSY correlations are shown in Figure 2. In addition, an oxide ethylene group was proposed at C-4 (δ_C 55.8) and C-29 (δ_C 63.7), as supported by published reports.(38) Accordingly, the planar structure of **3** is established as shown. Compound **3** proved to be a mixture of two isomers, **3a** and **3b**, since the ^{1}H and ^{13}C NMR data displayed two sets of signals (Table 1) with a relative ratio of 1.0:1.2, respectively. These isomers have four stereocenters (C-6, C-30, C-4, and C-29); two of them, C-4 and C-29, have the same stereochemistry since they are supporting the epoxide group. The signals at δ_H 4.00 (d, J = 1.2 Hz, H-30) and 4.27 (d, J = 1.2 Hz, H-29) for **3a** and δ_H 3.96 (d, J = 1.2 Hz, H-30) and 4.28 (d, J = 1.3 Hz, H-29) for **3b** supported the orientation of stereocenters C-4/29 and C-30 as *R,R,R* or *S,S,S*. This was in agreement with the dihedral angle ($^3J_{HCCH} = -114°$) between H-29 and H-30 obtained by the 3D models generated for each isomer (data not shown). Due to the paucity of sample, it was impossible to establish the absolute stereochemistry of these isomers.

Paucinone H (**4**) was purified from peak *l*, and the HRQTOFMS showed a molecular ion at *m/z* 549.2852 $[H + M]^+$ (calcd for 549.2852, $C_{33}H_{41}O_7$), consistent with a molecular formula of $C_{33}H_{40}O_7$, with 14 degrees of unsaturation. Similar to **3**, compound **4** was found to be an isomeric mixture of **4a** and **4b** with a relative ratio of 1.0:1.6, respectively, based on the ^{1}H and ^{13}C NMR data (Table 2). The spectroscopic data of **4** were similar to those of **3**, except for C-30 (**4**: δ_C 38.0, δ_H 2.64 and 2.56; **3**: δ_C 70.9, δ_H 4.00), indicating that C-30 of **4** is an sp^3 methylene with the hydroxy group signal in **3** missing from **4**. The key ^{1}H–^{1}H COSY and HMBC correlations of **4** were the same as **3**. Therefore, the above evidence was used to propose the planar structure of **4**. Since C-30 is not chiral, there is no experimental data to support the relative orientation of C-4 and C-29. Compound **4** was isolated in limited amounts, so the absolute stereochemistry could not be determined experimentally.

Table 2. NMR Spectroscopic Data (300 MHz, CD_3OD) for Compounds 4 and 5

	4a		4b		5	
position	δ_C	δ_H (J in Hz)	δ_C	δ_H (J in Hz)	δ_C	δ_H (J in Hz)
1	197.7		197.7		212.8	
2	128.5		128.4		115.3	
3	166.2		166.0		181.8	
4	53.0		52.9		202.2	
5	205.5		205.3		56.4	
6	66.8		66.7		34.5	2.38, d (7.3)
7	35.5	2.45, 2.25, m	35.5	2.44, 2.22, m	119.9	5.04, m
8	119.4	4.99, m	119.3	4.98, m	140.0	
9	141.3		141.0		41.2	1.97, 1.88, m
10	41.2	2.02, 1.96, m	41.1	2.02, 1.96, m	27.9	2.10, m
11	28.1	2.09, 1.99, m	27.8	2.08, 1.93, m	125.4	5.03, m
12	125.2	5.11, m	125.0	5.10, m	132.4	
13	132.6		132.7		26.0	1.62, s
14	26.1	1.69, s	26.1	1.66, s	17.9	1.54, s
15	18.0	1.59, s	18.0	1.59, s	16.4	1.59, s
16	16.8	1.57, s	16.6	1.55, s	34.3	2.38, m

	4a		4b		5	
position	δ_C	δ_H (*J* in Hz)	δ_C	δ_H (*J* in Hz)	δ_C	δ_H (*J* in Hz)
17	39.0	2.67, 2.50, m	38.9	2.66, 2.49, m	120.1	5.04, m
18	119.0	5.03, m	118.7	5.02, m	135.9	
19	137.4		137.7		26.3	1.64, s
20	18.2	1.55, s	18.2	1.54, s	18.0	1.59, s
21	26.3	1.70, s	26.3	1.70, s	194.5	
22	193.6		193.6		132.4	
23	130.6		130.6		117.2	7.35, d (1.9)
24	116.3	7.37, d (2.1)	116.2	7.36, d (1.9)	146.2	
25	147.0		147.0		151.8	
26	153.2		153.2		115.3	6.71, d (8.2)
27	115.8	6.77, d (8.3)	115.7	6.76, d (8.3)	125.5	7.25, dd (8.3, 1.9)
28	125.4	7.19, dd (8.3, 2.1)	125.2	7.18, dd (8.3, 2.1)		
29	61.0	4.28, m	60.8	4.26, m		
30	38.0	2.64, 2.56, m	37.7	2.63, 2.52, m		
31	83.6		83.5			
32	31.2	1.16	31.2	1.16, s		
33	29.7	1.41	29.6	1.41, s		

In addition, **3** and **4** are similar structures, which was also supported by UPLC-QTOFMS^E analysis, since the compounds exhibit similar fragment peaks (Figure S1, Supporting Information).

Paucinone I (**5**), an orange powder, was obtained from peak *b*. The HRQTOFMS molecular ion peak at *m*/*z* 453.2279 $[H + M]^+$ (calcd for 453.2279, $C_{27}H_{33}O_6$) corresponded to its molecular formula of $C_{27}H_{32}O_6$, with 12 degrees of unsaturation. The ^{1}H NMR spectrum displayed signals for a trisubstituted aromatic ring [δ 7.35 (1H, d, *J* = 1.9 Hz), 7.25 (1H, dd, *J* = 8.3, 1.9 Hz), and 6.71 (1H, d, *J* = 8.2 Hz)], and five methyl groups [δ_H 1.54 (3H, s), 1.59 (6H, br s), 1.62 (3H, s), and 1.64 (3H, s)]. The ^{13}C NMR of **5** showed 27 carbon signals, assigned to three carbonyl carbons, five methyl groups, four methylenes, six methines, and nine quaternary carbons (Table 2). These NMR data were generally similar to those of **3**, which, supported by the key HMBC correlations of H-6/C-1, C-4, C-5, C-8; H-9/C-7, C-8, C-15; H-16/C-1, C-4, C-5, C-18; and H-23/C-21, H-27/C21, respectively (Figure 2), indicate that a geranyl group and a prenylated unit are attached to C-5 and a trisubstituted aromatic ring is linked to carbonyl carbon (C-21, δ_C 194.5). The remaining two carbons (C-2 and C-3) along with C-1, C-4, and C-5 constituted a pentacyclic structure. The hydroxy group is attached at C-3, as demonstrated by the high chemical shift at δ_C 181.8. The above evidence was used to elucidate the planar structure of **5**. The configuration at C-5 was established unequivocally by comparing the specific rotation value with that obtained through molecular modeling calculations for the enantiomers C-5*S* and C-5*R*, following the same protocol described for compounds **1** and **2** using the Gaussian 09 program (Figure S4, Supporting Information). Comparison of the experimental ($[\alpha]^{25}_D = -27$) and the calculated ($[\alpha]^{25}_D = -22$) specific rotation values allowed the absolute configuration of compound **5** to be determined as 5*S*.

The five isolated compounds (**1**–**5**) were evaluated for cytotoxicity against human breast cancer cells using a WST assay. Three cancer cell lines, MDA-MB-231, SKBR3, and MCF-7, were used for this study. However, none of the compounds tested were deemed cytotoxic for any of the cell lines used ($IC_{50} < 10$ μM).

Experimental Section

General Experimental Procedures

Optical rotations were measured on an Autopol IV polarimeter (Rudolph Research Analytical, Hackettstown, NJ, USA) equipped with a sodium lamp (589 nm) and a 10 cm microcell. UV spectra were recorded on a Evolution 300 UV–vis spectrometer (Thermo Scientific). IR spectra were measured on a Nicolet iS10 (Thermo Scientific). ECD spectra were determined using a circular dichroism spectrometer model 202–-01 (Aviv Biomedical, Lakewood, NJ, USA) and recorded at 589 nm from 25 °C using 1 mm quartz cells. A Bruker Avance 300 NMR spectrometer was operated at 300.1312 MHz for ^{1}H and at 75.4753 MHz for ^{13}C NMR experiments. UPLC-QTOFMS was operated using an Acquity UPLC system (Waters Corporation, Milford, MA, USA) coupled with a QTOF-MS (Xevo G2 QTOF, Waters MS Technologies, Manchester, UK), controlled by MassLynx v4.1 software. HPLC separations used a Waters 2695 separation module, equipped with a Waters 2996 photodiode array detector, with an HPLC column (Synergi 4 μm Hydro-RP 80 Å, 250 × 4.6 mm, Phenomenex) for analysis, while semipreparative HPLC was carried out on an Econosil C_{18} column (10 μm, 250 × 10 mm, Grace Alltech). Sephadex LH-20 (25–100 μm, Pharmacia Fine Chemicals, Piscataway, NJ, USA) and HPLC-MS grade acetonitrile, water, and formic acid were purchased from J. T. Baker (Philipsburg, NJ, USA). Thin-layer chromatography silica gel plates and silica gel 200–300 mesh (Qingdao Haiyang Chemical Co. Ltd. Qingdao, People's Republic of China) were used, and all reagents were analytical grade (Beijing Chemical Works, Beijing, People's Republic of China).

Plant Material

Garcinia paucinervis seeds were collected in July 2014 from Xishuangbanna, Yunnan Province, in People's Republic of China, and the specimens were identified by one of the authors (C.L.L.). The voucher specimens (herbarium no. 20144538) were deposited in the Herbarium of Minzu University of China in Beijing, People's Republic of China.

Extraction and Isolation

Air-dried *G. paucinervis* seeds (1 kg) were ground into a powder and extracted twice with 2 L of 95% ethanol soaked for 48 h. The filtered solution was concentrated under reduced pressure at 40 °C to yield a crude extract (320 g). Water (800 mL) was added to dissolve the crude extract. The same volume of petroleum ether was used for solvent–solvent partitioning, and the upper phase (petroleum extract) was removed (140 g). The residue (120 g) was purified by silica gel column chromatography (120 × 10 cm), eluted with a gradient solvent system of petroleum ether–acetone (100:0 → 0:100, 800 mL collected volumes of each fraction), and concentrated, affording nine combined fractions (Fr. A–Fr. I, 0.5, 2.2, 2.1, 1.5, 2.0, 7.8, 13.2, 5.1, and 6.0 g, respectively). Each fraction was then analyzed by UPLC-QTOFMS before preparative-scale isolation work commenced.

Fraction D (1.0 g) was chromatographed over Sephadex LH-20 (150 × 2.5 cm, MeOH) to afford five subfractions (Fr. D_1–Fr. D_5). Fr. D_4 (280 mg) was subsequently purified by reversed-phase

preparative HPLC using gradient elution [MeCN–H_2O with 0.1% formic acid, 60:40 → 63:37 over 25 min] to obtain compound **3** (t_R: 15 min, 20 mg) and compound **4** (t_R: 22 min, 10.5 mg). Compound **3** was further purified by analytical HPLC with isocratic elution [MeCN–H_2O (52:48)], with a flow rate of 1.5 mL/min, to yield 12.5 mg (t_R: 26 min). Fraction E (250 mg) was purified by semipreparative HPLC with isocratic elution [MeCN/H_2O with 0.1% formic acid (45:55)] with a flow rate of 3 mL/min, yielding compounds **1** (t_R: 27 min, 18.0 mg) and **2** (t_R: 31 min, 12.0 mg). Fraction I (700 mg) was chromatographed over Sephadex LH-20 (150 × 2.5 cm) to give six subfractions (Fr. I_1–Fr. I_6). Fr. I_3 (200 mg) was repeatedly chromatographed by reversed-phase HPLC, eluting with a step gradient from 65% to 70% MeOH, giving compound **5** (t_R: 10 min, 15.0 mg).

Paucinone E (1):

yellow, amorphous powder; $[\alpha]^{25}_D$ +66 (*c* 0.6, MeOH); UV (MeOH) λ_{max} (log ε) 204 (2.47), 260 (0.67), 287 (0.93) nm; ECD (MeOH, Δε) λ_{max} 236 (−36.2), 280 (+14.5) nm; IR (MeOH) ν_{max} 3317, 2944, 2832, 1449, 1115, 1022 cm^{-1}; ^1H and ^{13}C NMR (methanol-d_4, 300 MHz) data, see Table 1; HRESIMS *m*/*z* 645.3070 $[M + H]^+$ (calcd for $C_{38}H_{45}O_9$, 645.3064).

Paucinone F (2):

yellow, amorphous powder; $[\alpha]^{25}_D$ −74 (*c* 0.35, MeOH); UV (MeOH) λ_{max} (log ε) 205 (2.65), 260 (0.77), 285 (1.06) nm; ECD (MeOH, Δε) λ_{max} 236 (+50), 344 (−15.5) nm; IR (MeOH) ν_{max} 3315, 2943, 2831, 1449, 1115, 1022 cm^{-1}; ^1H and ^{13}C NMR (methanol-d_4, 300 MHz) data, see Table 1; HRESIMS *m*/*z* 645.3063 $[M + H]^+$ (calcd for $C_{38}H_{45}O_9$, 645.3064).

Paucinone G (3):

yellow, amorphous powder; UV (MeOH) λ_{max} (log ε) 205 (2.58), 236 (1.63), 275 (1.64) nm; IR (MeOH) ν_{max} 3316, 2943, 2831, 1449, 1115, 1022 cm^{-1}; ^1H and ^{13}C NMR (methanol-d_4, 300 MHz) data, see Table 1; HRESIMS *m*/*z* 565.2803 $[M + H]^+$ (calcd for $C_{33}H_{41}O_8$, 565.2801).

Paucinone H (4):

yellow, amorphous powder; UV (MeOH) λ_{max} (log ε) 204 (2.33), 235 (1.30), 277 (1.24) nm; IR (MeOH) ν_{max} 3312, 2943, 2831, 1449, 1115, 1022 cm^{-1}; ^1H and ^{13}C NMR (methanol-d_4, 300 MHz) data, see Table 2; HRESIMS *m*/*z* 549.2849 $[M + H]^+$ (calcd for $C_{33}H_{41}O_7$, 549.2852).

Paucinone I (5):

orange, amorphous powder; $[\alpha]^{25}_D$ −27 (*c* 0.22, MeOH); UV (MeOH) λ_{max} (log ε) 206 (2.83), 251 (0.70), 283 (1.32), 321 (1.14) nm; IR (MeOH) ν_{max} 3312, 2943, 2831, 1449, 1115, 1022 cm^{-1}; ^1H and ^{13}C NMR (methanol-d_4, 300 MHz) data, see Table 2; HRESIMS *m*/*z* 453.2278 $[M + H]^+$ (calcd for $C_{27}H_{33}O_6$, 453.2277).

UPLC-QTOFMS Analysis

Chromatographic separation was performed with a 2.1 × 50 mm i.d., 1.7 μm UPLC BEH C_{18} reversed-phase column and kept at a temperature of 40 °C. The mobile phase consisted of 0.1% aqueous formic acid (A) and 0.1% formic acid in acetonitrile (B). The linear gradient elution was performed as follows: 0–0.5 min, 20% B; 0.5–2.5 min, 20–65% B; 2.5–5 min, 65–70% B; 5–7.5 min, 70–75% B; 7.5–11.0 min, 75–95% B; 11.0–12.8 min, 95–95% B; 12.8–13.2 min, 95–20% B; 13.2–15.0 min, 20–20% B. A flow rate of 0.4 mL/min was employed for elution, and the injected sample (2 mg/mL) volume was set at 1 μL. Mass spectrometry was recorded using a Xevo G2 QTOF equipped with an ESI source and controlled by MassLynx v4.1 software. The MS and MS^E data resolution modes of scans were applied. MS full scanning was conducted in both positive ion and negative ion modes over the range *m*/*z* 100–1000 Da in two channels, with a scan time of 0.5 s. The capillary voltages were set at 3100 V (positive mode) and 2500 V (negative mode), respectively, and the cone voltage was 20 V. Nitrogen gas was used both for the nebulizer and in desolvation. The desolvation and cone gas flow rates were 600 and 20 L/h, respectively. The desolvation temperature was 400 °C, and the source temperature was 120 °C. The MS^E experiments were conducted in the centroid configuration in the positive mode, with a range of *m*/*z* 50–1000 Da, and survey scan time was 0.5 s, the low energy was set as 5 V, while the high energy was ramped from 25 to 50 V. The cone voltage was set as 60 V. The lock mass solution of leucine enkephalin (1 μg/mL) in acetonitrile–water (1:1) containing 0.1% formic acid was utilized as the lock mass at a flow rate of 10 μL/mL, with *m*/*z* 556.2771 for the positive mode and *m*/*z* 554.2615 for the negative mode.

Molecular Modeling Calculations

Theoretical calculations of ECD spectra for diasteroisomers **1** and **2** were performed with the Gaussian 09 (Gaussian Inc., Wallingford, CT, USA) program package as described previously.(27, 33-36) Briefly, geometry optimizations and conformer distribution analysis for all structures were carried out using the MMFF94 molecular mechanics force field calculations as implemented in the Spartan 08 program (Wavefunction Inc., Irvine, CA, USA).(39) A Monte Carlo search protocol(40) was carried out considering an energy cutoff of 5 kcal/mol. For each structure, all minimum energy conformers were filtered and checked for duplicity and then geometrically optimized using the hybrid DFT method B3LYP and the basis set DGDZVP (B3LYP/DGDZVP), with thermochemical parameters and frequencies at 298 K and 1 atm. Their thermochemical properties, optical rotation, IR, and vibrational analyses were calculated at the same level. The self-consistent reaction field method (SCRF) with the conductor-like screening model (COSMO) was employed to perform the ECD calculations of major conformers for each compound in their respective solvent solution with the same basis set. The calculated excitation energy (in nm) and rotatory strength *R*, in dipole velocity (R_{vel}) and dipole length (R_{len}) forms, were simulated into an ECD curve by using the following Gaussian function:

$$\Delta\varepsilon(E) = \sum_{i=1}^{n} \Delta\varepsilon_i(E) = \sum_{i=1}^{n} \left(\frac{R_i E_i}{2.29 \times 10^{-39} \sqrt{\pi\sigma}} \exp\left[-\left(\frac{E - E_i}{\sigma} \right) \right] \right)$$

where σ is the width of the band at 1/*e* height and E_i and R_i are the excitation energies and rotatory strengths for transition *i*, respectively. σ = 0.40 eV and R_{vel} were used. The Boltzmann-averaged ECD spectra were obtained from B3LYP/DGDZVP-optimized structures. All quantum calculations were carried out on a Linux operating system in the KanBalam cluster from a Hewlett-Packard HP CP 4000, which includes 1368 AMD Opteron processors at 2.6 GHz and a RAM memory of 3 terabytes (KanBalam, Dirección General de Cómputo y de Tecnologías de Información y Comunicación, UNAM,

Mexico City, Mexico). For each task, up to 16 processors were used, and each conformer required three different DFT tasks: geometric optimizations, frequency calculations, and TD ECD calculations. The free energy equation ($\Delta G = -RT \ln K$) was used to obtain the conformational population, taking into account a cyclic equilibrium at 298 K between the selected conformers of each structure within a 0.0–5.0 kcal/mol window with respect to the global minimum. The free energy values $\Delta G°$ were obtained from the vibrational frequency calculations as the sum of electronic and thermal free energies.

Growth Inhibitory Effects on a Panel of Breast Cancer Cells

All compounds tested in vitro were dissolved in DMSO and diluted with required volumes of respective cell culture media before each treatment. The volume of DMSO did not exceed 0.001% in the wells after treatment. MDA-MB-231 and MCF7 cells were cultured in DMEM glucose medium (Gibco, USA) supplemented with 10% fetal calf serum and 100 μL of antibiotics (penicillin and streptomycin). SKBR3 cells were cultured in DMEM F12 glutamine medium supplemented with 10% fetal calf serum and 100 μL of antibiotics (penicillin and streptomycin). All cells were maintained at 37 °C in an incubator with 5% CO_2. To determine the cytotoxicity effects of the test compounds on the three cell lines mentioned above, exponentially growing cells (12×10^3 cells/well) were seeded in 96-well multitier plates. After 24 h, each test compound was added to each cell line used for this study. Concentrations of the compounds studied ranged from 5 to 200 μM. Doxorubicin was used as a positive control. After 48 h treatment, a cell viability assay (WST) was performed. Each well was washed twice with serum-free medium followed by the addition of a 10% WST solution. This solution (150 μL) was then added to each well. The plates were wrapped in aluminum foil and incubated for 1 h; their absorbance was then read at 440 nm using a Spectra Max plate reader. Each experiment was performed in triplicate. Average absorbance and the percentage inhibition relative to the control were calculated. The results were analyzed using Graph Pad Prism Software (Graph Pad Software, San Diego, CA, USA), and IC_{50} values were estimated.

Supporting Information

The Supporting Information is available free of charge on the ACS Publications website at DOI: 10.1021/acs.jnatprod.6b00186.

The authors declare no competing financial interest.

Acknowledgment

The authors wish to thank Dr. Y. Xu, Hunter College, CUNY, for measuring ECD spectra of compounds; Dr. B. Zajc, City College, CUNY, for acquiring the optical rotation data; and Ms. J. Kwok for culturing cell lines. Dr. B. Liu and Dr. W. Cao from Minzu University of China are recognized for carrying out field work and harvesting the plant material used in this study. We would also like to thank the Dirección General de Cómputo y de Tecnologías de Información y Comunicación (DGTIC-UNAM) for providing the resources to carry out computational calculations through the KanBalam system. This work was supported by the Ministry of Education of China through its 111 Program and the Discipline Development Program for Minzu

University of China (B08044, YLDX01013, and 2015MDTD16C), the National Natural Science Foundation of China (3116140345 and 31070288), the China Scholarship Council (CSC), and the Graduate Research and Innovation Project of Minzu University of China (Z2014045). Support was also provided by a CUNY Collaborative grant to J.E.F. and E.J.K.

References

1. Wu, S. B.; Long, C.; Kennelly, E. J. Nat. Prod. Rep. **2014**, 31, 1158– 1174 DOI: 10.1039/C4NP00027G

2. Ciochina, R.; Grossman, R. B. Chem. Rev. **2006**, 106, 3963– 3986 DOI: 10.1021/cr0500582

3. Kumar, S.; Sharma, S.; Chattopadhyay, S. K. Fitoterapia **2013**, 89, 86– 125 DOI: 10.1016/j.fitote.2013.05.010

4. Fu, Y.; Zhou, H.; Wang, M.; Cen, J.; Wei, Q. J. Agric. Food Chem. **2014**, 62, 4127– 4134 DOI: 10.1021/jf405790q

5. Yamaguchi, F.; Saito, M.; Ariga, T.; Yoshimura, Y.; Nakazawa, H. J. Agric. Food Chem. **2000**, 48, 2320– 2325 DOI: 10.1021/jf990908c

6. Liu, X.; Yu, T.; Gao, X. M.; Zhou, Y.; Qiao, C. F.; Peng, Y.; Chen, S. L.; Luo, K. Q.; Xu, H. X. J. Nat. Prod. **2010**, 73, 1355– 1359 DOI: 10.1021/np100156w

7. Feng, C.; Huang, S. X.; Gao, X. M.; Xu, H. X.; Luo, K. Q. J. Nat. Prod. **2014**, 77, 1111– 1116 DOI: 10.1021/np4007316

8. Acuña, U. M.; Jancovski, N.; Kennelly, E. J. Curr. Top. Med. Chem. **2009**, 9, 1560– 1580 DOI: 10.2174/156802609789909830

9. Fan, Y. M.; Yi, P.; Li, Y.; Yan, C.; Huang, T.; Gu, W.; Ma, Y.; Huang, L. J.; Zhang, J. X.; Yang, C. L. Org. Lett. **2015**, 17, 2066– 2069 DOI: 10.1021/acs.orglett.5b00588

10. Zhou, Y.; Huang, S. X.; Song, J. Z.; Qiao, C. F.; Li, S. L.; Han, Q. B.; Xu, H. X. J. Am. Soc. Mass Spectrom. **2009**, 20, 1846– 1850 DOI: 10.1016/j.jasms.2009.06.008

11. Stark, T. D.; Losch, S.; Wakamatsu, J.; Balemba, O. B.; Frank, O.; Hofmann, T. J. Agric. Food Chem. **2015**, 63, 7169– 7179 DOI: 10.1021/acs.jafc.5b02544

12. Abad-Garcia, B.; Berrueta, L. A.; Garmon-Lobato, S.; Gallo, B.; Vicente, F. J. Chromatogr. A **2009**, 1216, 5398– 5415 DOI: 10.1016/j.chroma.2009.05.039

13. Yang, M.; Sun, J.; Lu, Z.; Chen, G.; Guan, S.; Liu, X.; Jiang, B.; Ye, M.; Guo, D. A. J. Chromatogr. A **2009**, 1216, 2045– 2062 DOI: 10.1016/j.chroma.2008.08.097

14. Nielsen, K. F.; Mansson, M.; Rank, C.; Frisvad, J. C.; Larsen, T. O. J. Nat. Prod. **2011**, 74, 2338– 2348 DOI: 10.1021/np200254t

15. Piccinelli, A. L.; Campone, L.; Dal Piaz, F.; Cuesta-Rubio, O.; Rastrelli, L. J. Am. Soc. Mass Spectrom. **2009**, 20, 1688– 1698 DOI: 10.1016/j.jasms.2009.05.004

16. Zhou, Y.; Lee, S.; Choi, F. F.; Xu, G.; Liu, X.; Song, J. Z.; Li, S. L.; Qiao, C. F.; Xu, H. X. Anal. Chim. Acta **2010**, 678, 96– 107 DOI: 10.1016/j.aca.2010.08.010

17. Wrona, M.; Mauriala, T.; Bateman, K. P.; Mortishire-Smith, R. J.; O'Connor, D. Rapid Commun. Mass Spectrom. **2005**, 19, 2597– 2602 DOI: 10.1002/rcm.2101

18. Plumb, R. S.; Johnson, K. A.; Rainville, P.; Smith, B. W.; Wilson, I. D.; Castro-Perez, J. M.; Nicholson, J. K. Rapid Commun. Mass Spectrom. **2006**, 20, 1989– 1994 DOI: 10.1002/rcm.2550

19. Ramirez-Ambrosi, M.; Abad-Garcia, B.; Viloria-Bernal, M.; Garmon-Lobato, S.; Berrueta, L. A.; Gallo, B. J. Chromatogr. A **2013**, 1316, 78– 91 DOI: 10.1016/j.chroma.2013.09.075

20. Fan, Q.; Na, Z.; Hu, H.; Xu, Y.; Tang, T. Chin. Trad. Herbal Drugs **2012**, 43, 436– 439

21. Gao, X. M.; Yu, T.; Lai, F. S. F.; Pu, J. X.; Qiao, C. F.; Zhou, Y.; Liu, X.; Song, J. Z.; Luo, K. Q.; Xu, H.-X. Tetrahedron Lett. **2010**, 51, 2442– 2446 DOI: 10.1016/j.tetlet.2010.02.147

22. Wu, Y. P.; Zhao, W.; Xia, Z. Y.; Kong, G. H.; Lu, X. P.; Hu, Q. F.; Gao, X. M. Molecules **2013**, 18, 9663– 9669 DOI: 10.3390/molecules18089663

23. Gao, X. M.; Yu, T.; Lai, F. S.; Zhou, Y.; Liu, X.; Qiao, C. F.; Song, J. Z.; Chen, S. L.; Luo, K. Q.; Xu, H. X. Bioorg. Med. Chem. **2010**, 18, 4957– 4964 DOI: 10.1016/j.bmc.2010.06.014

24. Baggett, S.; Protiva, P.; Mazzola, E. P.; Yang, H.; Ressler, E. T.; Basile, M. J.; Weinstein, I. B.; Kennelly, E. J. J. Nat. Prod. **2005**, 68, 354– 360 DOI: 10.1021/np0497595

25. Protiva, P.; Hopkins, M. E.; Baggett, S.; Yang, H.; Lipkin, M.; Holt, P. R.; Kennelly, E. J.; Bernard, W. I. Int. J. Cancer **2008**, 123, 687– 694 DOI: 10.1002/ijc.23515

26. Yang, H.; Figueroa, M.; To, S.; Baggett, S.; Jiang, B.; Basile, M. J.; Weinstein, I. B.; Kennelly, E. J. J. Agric. Food Chem. **2010**, 58, 4749– 4755 DOI: 10.1021/jf9046094

27. Acuña, U. M.; Figueroa, M.; Kavalier, A.; Jancovski, N.; Basile, M. J.; Kennelly, E. J. J. Nat. Prod. **2010**, 73, 1775– 1779 DOI: 10.1021/np100322d

28. Einbond, L. S.; Mighty, J.; Kashiwazaki, R.; Figueroa, M.; Jalees, F.; Acuna, U. M.; Le Gendre, O.; Foster, D. A.; Kennelly, E. J. Anti-Cancer Agents Med. Chem. **2013**, 13, 1540– 1550 DOI: 10.2174/18715206113139990095

29. Chiang, Y. M.; Kuo, Y. H.; Oota, S.; Fukuyama, Y. J. Nat. Prod. **2003**, 66, 1070– 1073 DOI: 10.1021/np030065q

30. Raikar, S. B.; Nuhant, P.; Delpech, B.; Marazano, C. Eur. J. Org. Chem. **2008**, 2008, 1358– 1369 DOI: 10.1002/ejoc.200701009

31. Hussain, R. A.; Owegby, A. G.; Parimoo, P.; Waterman, P. G. Planta Med. **1982**, 44, 78– 81 DOI: 10.1055/s-2007-971406

32. Hashidoko, Y. Biosci., Biotechnol., Biochem. **1995**, 59, 886– 890 DOI: 10.1271/bbb.59.886

33. Bringmann, G.; Bruhn, T.; Maksimenka, K.; Hemberger, Y. Eur. J. Org. Chem. **2009**, 17, 2717– 2727 DOI: 10.1002/ejoc.200801121

34. Ding, Y.; Li, X. C.; Ferreira, D. J. Nat. Prod. **2009**, 72, 327– 335 DOI: 10.1021/np800146v

35. Stephens, P. J.; Harada, N. Chirality **2010**, 22, 229– 233 DOI: 10.1002/chir.20733

36. Stephens, P. J.; Pan, J. J.; Devlin, F. J.; Urbanova, M.; Hajicek, J. J. Org. Chem. **2007**, 72, 2508– 2524 DOI: 10.1021/jo062567p

37. Piao, S. J.; Jiao, W. H.; Yang, F.; Yi, Y. H.; Di, Y. T.; Han, B. N.; Lin, H. W. Mar. Drugs **2014**, 12, 4096– 4109 DOI: 10.3390/md12074096

38. Yurchenko, A. N.; Smetanina, O. F.; Khudyakova, Y. V.; Kirichuk, N. N.; Chaikina, E. L.; Anisimov, M. M.; Afiyatullov, S. S. Chem. Nat. Compd. **2013**, 49, 857– 860 DOI: 10.1007/s10600-013-0764-0

39. Kong, J.; White, C. A.; Krylov, A. I.; Sherrill, D.; Adamson, R. D.; Furlani, T. R.; Lee, M. S.; Lee, A. M.; Gwaltney, S. R.; Adams, T. R.; Ochsenfeld, C.; Gilbert, A. T. B.; Kedziora, G. S.; Rassolov, V. A.; Maurice, D. R.; Nair, N.; Shao, Y.; Besley, N. A.; Maslen, P. E.; Dombroski, J. P.; Daschel, H.; Zhang, W.; Korambath, P. P.; Baker, J.; Byrd, E. F. C.; Van Voorhis, T.; Oumi, M.; Hirata, S.; Hsu, C.-P.; Ishikawa, N.; Florian, J.; Warshel, A.; Johnson, B. G.; Gill, P. M. W.; Head-Gordon, M.; Pople, J. A. J. Comput. Chem. **2000**, 21, 1532– 1548 DOI: 10.1002/1096-987X(200012)21:16<1532::AID-JCC10>3.0.CO;2-W

40. Chang, G.; Guida, W. C.; Still, W. C. J. Am. Chem. Soc. **1989**, 111, 4379– 4386 DOI: 10.1021/ja00194a035